

# Multi-Melting Behavior and Glass Transition of Monotropic Polymorphs of 3,5-Diphenyl-4-hydroxyphenyl Substituted Galvinol

Mai Takahashi, Hiroki Ogino, and Keiji Kobayashi\*

Josai University, Graduate School of Material Science, Keyakidai 1-1, Sakado, Saitama, 350-0295

(Received <Month> <Date>, <Year>; CL-<No>; E-mail: <insert corresponding e-mail address>)

A galvinol derivative bearing the 3,5-diphenyl-4-hydroxyphenyl substituent exists in three polymorphic forms, *i.e.*, **I** (melting point, 208 °C), **II** (203 °C), and **III** (138 °C), which are interrelated as monotropic polymorphs. Of these forms, **III** exhibits multiple melting behavior. The relative thermodynamic stability of the three forms was determined and is represented in a semi-schematic energy/temperature diagram. All three forms, once melted and cooled, solidify to form glass with a glass transition temperature of 109 °C.

Multiple melting behavior has been studied mostly in flexible semicrystalline polymer systems<sup>1</sup> and attributed to various factors including pre-existing multiple crystal structures and the reorganization of previously less ordered structures.<sup>2</sup> They may also be observed in inorganic complexes bearing multiple eutectic points.<sup>3</sup> In these materials, the coexistence of multiple kinds of crystalline modification is responsible for multi-melting. On the other hand, low-molecular-weight molecular crystals hardly exhibit multi-melting behavior.<sup>4</sup> Herein, we demonstrate a peculiar multi-melting phenomenon recognized for a low-molecular-weight organic compound, which is achieved by heating a less stable modification of monotropically related polymorphs. For monotropic polymorphs,<sup>5</sup> the same polymorph can be stable over the entire temperature range up to the melting point in contrast to enantiotropic polymorphs, where, at a certain temperature, two polymorphs are in equilibrium. In a monotropic system, all phase transitions are irreversible, that is, a less stable polymorph can change into a more stable one; in an enantiotropic system, a reversible interconversion of two polymorphs upon heating and cooling is possible. When a less stable form of a monotropic polymorph could be obtained, heating its crystals might induce melting and spontaneous recrystallization from melts to generate a more stable form; hence, a multi-melting is realized. In spite of the fundamental concepts of monotropic polymorphs, however, such phenomena are often overlooked, since heating crystals above their melting temperature is usually not conducted.

The compound studied is (3,5-di-*t*-butyl-4-hydroxyphenyl)-(3,5-di-phenyl-4-hydroxyphenyl)methylene-2,6-di-*t*-butyl-2,5-cyclohexadien-1-one (**1**), which was prepared by the reaction of galvinol and 2,6-diphenylphenol, with the intention of exploring a new Yang's diradical precursor.<sup>6</sup> The molecular structure of **1** was elucidated by an X-ray crystallographic study for a single crystal of form **I** (Figure 1),<sup>7</sup> which was obtained by the recrystallization of **1** from heptanes. One of the *t*-butyl-substituted six-membered rings exists as a quinonoid framework, as judged from alternating carbon-carbon bond lengths of the ring<sup>8</sup> and from the distinct

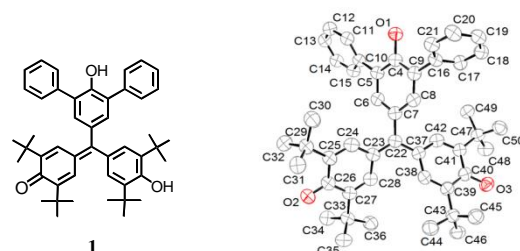


**Figure 1.** Chemical structure of **1** and ORTEP drawing of the molecular structure of **1** in the crystal form **I**. Hydrogen atoms are omitted for clarity.

carbon-oxygen bond lengths.<sup>9</sup> The <sup>1</sup>H NMR result is in good accord with the structure determined by X-ray analysis (Figure S1 in Supporting Information).<sup>10</sup> Thus, the molecular structure in the crystalline state is apparently retained in solution.<sup>11</sup>

The DSC traces of form **I**, the form with the highest melting point among the three polymorphs, display only an endothermic peak at 208 °C accompanied by an enthalpy of melt  $\Delta H_m$  of 48.2 kJ/mol (Figure S2, Table 1).<sup>12</sup> When recrystallized from methanol/acetonitrile, **1** forms solvates (**1**) (MeOH)<sub>2</sub>, which easily release solvent molecules to form **III**, a solvent-free microcrystalline solid form of **1**. Desolvation is accompanied by a broad endothermic DSC peak, which ranges from room temperature to about 90 °C with the peak top at 81 °C (Figure 2). The **1**:MeOH ratio was determined by <sup>1</sup>H NMR spectroscopy as well as thermogravimetric analysis indicating a mass loss of 8.6% (Figure S3). The DSC of **III** occurs in unexpected profiles, producing a new solid phase, **II**, and hence, inducing double melting behavior. Thus, the DSC traces of **III** exhibits the melting endotherm of **III** at 138 °C

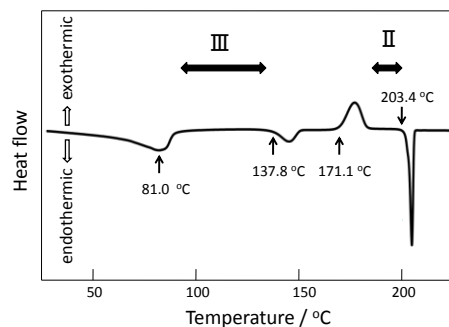


**Figure 2.** DSC curves for solvated crystals of (**1**) (MeOH)<sub>2</sub> recorded at 2 °C/min rate, showing the temperature range for the occurrence of polymorphs **III** and **II**.

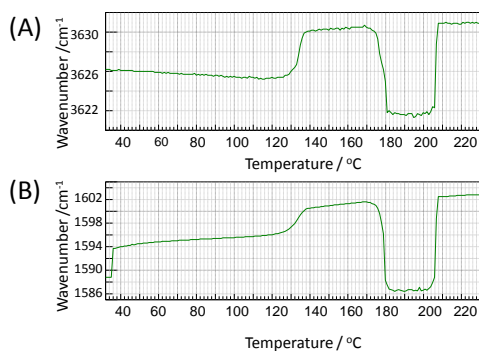


**Figure 3.** Peak shifts in FT-IR spectra during heating of **III** from room temperature to 230 °C. (A) 3626  $\text{cm}^{-1}$  peak. (B) 1594  $\text{cm}^{-1}$  peak.

and then a solidification exotherm at 171 °C to produce **II**. **II** melts at 203 °C and therefore exists only in a relatively narrow temperature range of 180 - 200 °C. Thus, **II** could be collected by heating **III** at a constant temperature of 190 °C on a hot plate.

In accord with the results of DSC analysis, the variable-temperature microscopic FTIR spectra of **III** indicate distinct changes in peak positions with increasing temperature. Figure 3 shows the wavenumber shifts of the O-H and C=O absorption bands, which were measured at a heating rate of 2 °C/min, the same rate used for the DSC analysis with the intention of simultaneously performing IR and DSC analysis. Thus, corresponding to the phase transition observed in the DSC traces, the peak positions exhibit abrupt shifts due to melting and the reorganization of crystal structures. For example, the 3626  $\text{cm}^{-1}$  peak of **III** at 40 °C, assigned to the OH stretching mode, shifts to a higher wavelength in **II** at 138 °C owing to melting, and changes to 3621  $\text{cm}^{-1}$  at 171 °C by solidification to **II**; with further heating, **II** reverts to the melt phase [Figure 3(A)]. The peak of the melt phase appears twice during heating up to 220 °C, which occurs as a steady upward shift with increasing temperature, probably ascribed to the thermal expansion of the liquid phase. Similar changes in wavenumber are also observed for the C=O band of 1594  $\text{cm}^{-1}$  [Figure 3(B)].

The X-ray powder reflections (XRD) of **I**, **II**, and **III** are different from each other (Figure S4) and, as noted above, their IR spectra are also different; however, the  $^1\text{H}$  NMR spectra in  $\text{C}_6\text{D}_{12}$  are the same, representing the structural formula of **I**. In the DSC heating of **II**, that is, the melt-recrystallized sample starting from **III**, only a single-melting endotherm at 207 °C is observed with no other phase transitions, indicating that **II** is more stable than **III** below its melting temperature and that their interconversion is irreversible. Therefore, **II** and **III** are interrelated as monotropic polymorphs. **I** and **II** are also monotonically related pairs, wherein higher-melting-point **I** is always the thermodynamically stable form: the DSC heating scan of **I** exhibits only a melting peak at 208 °C (Figure S2). The difference in melting temperature between **I** and **II** is only 5 °C, therefore, one might ask whether **I** and **II** are the same crystalline phase. From the XRD and IR profiles, however, these two phases are clearly different.<sup>13</sup> Furthermore, despite the very close melting points of **I** and **II**, their distinction is

**Table 1.** Melting temperatures ( $T_m$ ) of and enthalpy changes ( $\Delta H_m$ ) for polymorphs **I**, **II**, and **III**.

form	$T_m$ (onset) / °C	$T_m$ (peak top) / °C	$\Delta H_m$ / $\text{kJmol}^{-1}$
<b>I</b>	207.7	209.5	48.2
<b>II</b>	203.4	206.9	36.1
<b>III</b>	137.8	145.7	15.6

evident on the basis of the enthalpy of the melt ( $\Delta H_m$ ); the value follows the order **I** > **II** > **III** (Table 1), which confirms that **I** is the most stable polymorph among the three. A schematic energy-temperature diagram of these monotonically related polymorphs is shown in Figure 4. The second and third melting points are so close (with only a 5 °C difference), which would make it difficult for **I** to crystallize spontaneously from the melt of **II**. In fact, we are unable to experimentally observe the solidification and subsequent melting of **I**. However, a diagram clearly shows the virtual occurrence of a triple-melting event. The ultimate melting point experimentally observed as a result of heating **III** up to ca. 210 °C is not the melting point of **I** but actually of **II**. Once isolated by recrystallization from heptane, however, **I** exhibits its inherent melting point at 208 °C. Although the second solidification, which should occur between 203 and 208 °C, could not be observed, it is evident that **I** essentially exhibits triple-melting behavior.

The enthalpy of fusion, a measure of the lattice energy of a solid, well correlated with the conceivable crystallinity of all the solid forms obtained. **III**, resulting from the loss of solvent molecules, would be rather a unstable ‘nonperfect’ crystal with local disorder. It should be noticed that the first phase transition, that is, the melting of **III**, occurs gradually, as determined from the broad endothermic profile in DSC and the slow change of absorption peaks in IR, which is, in particular, observed in the C=O absorption at 1594  $\text{cm}^{-1}$  [Figure 3(B)]. These observations could be explained by the melting of nonperfect crystals of **III**.

Once the polymorphs **I**, **II**, and **III** melt and solidify with cooling, such melt-solidified samples exhibit noncrystallinity in the XRD profiles (Figure S5) and show the same thermal behavior regardless of their form. The DSC heating thermogram obtained at a rate of 2 °C/min is shown in Figure 5, which shows peaks A to C. Peak A at 109 °C

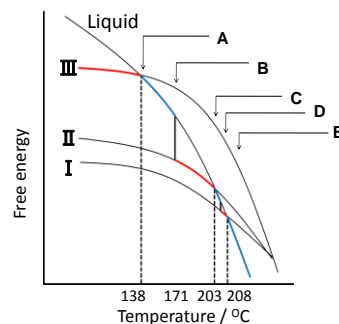


**Figure 4.** Semi-schematic free energy/temperature diagram for monotropic polymorphs **I**, **II**, and **III**. A: melt of **III**. B: crystallization of **II** from melt. C: melt of **II**. D: crystallization of **I** from melt. E: melt of **I**.

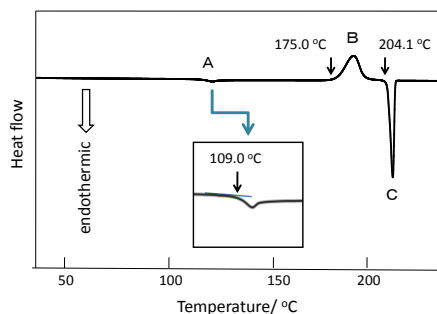


**Figure 5.** DSC heating curve for the melt-solidified samples of **I**, showing glass transition.

displays characteristic features of a glass transition, that is, a small peak due to enthalpy relaxation and a downward shift of the baseline. Peak B at 175 °C represents the crystallization of the supercooled liquid phase to the crystalline phase with an exothermic peak. With further heating, the crystal melts at 204 °C, as shown by peak C. The crystallization from the supercooled liquid phase occurs to form **II**, which is supported by the observation that the enthalpy of the melt of the resulting solids ( $\Delta H_m = 36.4 \text{ kJmol}^{-1}$ ) is comparable to that of **II** rather than that of **I**.

The supercooled phase lies over a significantly wide temperature range from 109 °C to 175 °C, and the formation of glass requires no rapid cooling. These observations indicate the difficulty in the crystallization of **1** owing to its irregular structure. Shirota et al. have developed low-molecular-weight organic glasses with a molecular shape of the star-burst type.<sup>14</sup> **1** may also be regarded as a kind of star-burst-type molecule. The molecular structure of **1** consists of highly congested substituents and rigid moiety subunits, which would be favorable for the crystallization in solvate crystals for more compact crystal lattices. The desolvation of solvate crystals could provide frequent chances to form monotropic polymorphs,<sup>15</sup> and such crystals themselves should be less stable polymorphic forms. Thus, multiple melting behavior would be realized in desolvated crystals. However, in most cases, these are missed without heating the crystals above the melting temperature. The present study reminds us of an important aspect, that is, multi-melting behavior should be more frequently discovered in monotropic polymorphs and could disclose new polymorphic forms that have not been identified thus far.

The authors gratefully acknowledge Dr. H. Sato, Rigaku Corporation, for the single-crystal X-ray analysis.

## References and Notes

1 For example, multi-melting behavior of poly(ethylene terephthalate) has been widely studied over the past 40 years. For recent leading reports: a) M. Yasuniwa, S. Tsubakihara, T. Murakami, *J. Polym. Sci. Part B: Polym. Phys.* **2000**, *38*, 262. b) M. Yasuniwa, S. Tsubakihara, K. Ohoshita, S. Tokudome, *J. Polym. Sci. Part B: Polym. Phys.* **2001**, *39*, 2005. c) Y. Kong, J. N. Hay, *Polymer* **2003**, *44*, 623. d) C. A. A-Orta, F. J. M-Rodriguez, Z-G. Wang, D. N-Rodriguetz, B. S. Hsiao, F. Yeh, *Polymer* **2003**, *44*, 1527.

- 2 a) N. Song, D. Yao, Z. Y. Wang, P. R. Sundararajan, *Polymer* **2005**, *46*, 3831. (b) T. Sasaki, H. Sunago, T. Hoshikawa, *Polym. Eng. Sci.* **2003**, *43*, 629. c) R. Caminiti, A. Isopo, M. A. Orru, V. R. Albertini, *Chem. Mater.* **2000**, *12*, 369.
- 3 A. Bogdan, M. J. Molina, H. Tenhu, T. Loerting, *Phys. Chem. Chem. Phys.* **2011**, *13*, 19704.
- 4 For recent examples; a) A. C. Schmidt, *J. Therm. Anal. Calori.* **2005**, *81*, 291. b) S. Cabus, K. Bogaerts, J. Van Mechelen, M. Smet, B. Goderis, *Cryst. Growth Des.* **2013**, *13*, 3438.
- 5 a) H. G. Brittain, *Methods for the Characterization of Polymorphs and Solvat Polymorphism in Pharmaceutical Solids*; H. G. Brittain Ed., Marcel Dekker, Inc. New York, 1999; pp 227-278. b) D. Giron, *Thermochimica Acta* **1995**, *248*, 1. c) A. Burger, R. Ramberger., *Mikrochim. Acta*, **1979**, *II*, 259.
- 6 N. C. Yang, A. J. Castro, *J. Am. Chem. Soc.* **1960**, *82*, 6208.
- 7 Crystallographic data for **1**:  $\text{C}_{47}\text{H}_{54}\text{O}_3$ , monoclinic, space group:  $C2/c$  (#15),  $a=46.408(4) \text{ \AA}$ ,  $b=5.7865(4) \text{ \AA}$ ,  $c=29.5127(17) \text{ \AA}$ ,  $\beta=90.188(6)^\circ$ ,  $V=7925.4(10) \text{ \AA}^3$ ,  $Z=8$ ,  $D_{\text{calcd}}=1.118 \text{ g/cm}^3$ ,  $T=-180 \text{ }^\circ\text{C}$ ,  $R1(I>2.00\sigma(I))=0.0781$ ,  $wR2(\text{all})=0.2429$ ,  $\text{GOF}=1.060$ .  $\text{CCDC}=959865$ .
- 8 Bond lengths for the quinonoid ring: C24-C25: 1.361(4)  $\text{ \AA}$ , C27-C-28: 1.369(4)  $\text{ \AA}$ , C25-C26: 1.444(4)  $\text{ \AA}$ , and C26-C27: 1.465  $\text{ \AA}$ .
- 9 Carbon-oxygen bond lengths: O1-C4: 1.374(3)  $\text{ \AA}$ , O2-C26: 1.288(3)  $\text{ \AA}$ , and O3-C40: 1.329(4)  $\text{ \AA}$ .
- 10 Supporting Information is available electronically on the CSJ-Journal website; <http://www.csj.jp/journals/chemlett/index.html>.
- 11 It is important to measure the NMR spectra of **1** using nonpolar solvents such as cyclohexane- $d_{12}$ . Otherwise, fast dynamic exchange of the OH protons will be induced.  $^1\text{H}$  NMR (700 MHz,  $\text{C}_6\text{D}_{12}$ ):  $\delta$  1.26 (s, 9H), 1.27 (s, 9H), 1.42 (s, 18H), 5.32 (s, 1H), 5.34 (s, 1H), 7.16 (s, 2H), 7.19 (s, 2H), 7.22 (d,  $J=3 \text{ Hz}$ , 1H), 7.25 (t,  $J=7 \text{ Hz}$ , 2H), 7.32 (d,  $J=3 \text{ Hz}$ , 1H), 7.33 (t,  $J=7 \text{ Hz}$ , 4H), 7.47 (d,  $J=7 \text{ Hz}$ , 4H).
- 12 Throughout the text and figures herein, the onset temperatures in the DSC profiles are indicated. The temperatures of the peak top are listed in Table 1.
- 13 Single crystals of **II** and **III** suited for X-ray analysis could not be obtained in spite of all our effort including seed growth crystallization.
- 14 a) E. Ueda, H. Nakano, Y. Shirota, *Chem. Lett.* **1994**, 2397. b) H. Kageyama, K. Itano, W. Ishikawa, Y. Shirota, *J. Mater. Chem.* **1996**, *6*, 675, and references cited therein.
- 15 A selected report, see: R. Chadha, P. Arora, M. Garg, S. Bhandari, D. S. Jain, *J. Therm. Anal. Calorim.* **2013**, *111*, 2133.